Dynamic response of marginal soil using SPT, DCPT & cyclic simple shear tests

Shrweta Dutta[1#], and *Ajanta* Sachan[2]

[1]*Ph.D. Student, Indian Institute of Technology Gandhinagar, Discipline of Civil Engineering, Gandhinagar, India*
[2]*Associate Professor, Indian Institute of Technology Gandhinagar, Discipline of Civil Engineering, Gandhinagar, India*
[#]*duttashrweta@iitgn.ac.in*

ABSTRACT

Coarse-grained soils are preferably used in geotechnical infrastructure projects such as retaining walls and highway embankments due to their superior drainage and frictional properties. However, such materials are not always available on or near the construction site. Given the limited availability, high cost, and transportation issues associated with coarse-grained fill, using the locally available marginal soil for the various infrastructure projects becomes essential. Marginal soils are soils with a high percentage of fines that can be cohesive or non-cohesive. The primary concern with marginal soil is its low permeability, which causes excess positive-pore water pressure evolution during load application. As a consequence, the soil loses shear strength over time. Previous researchers have provided some information on the dynamic behaviour of marginal soils in terms of cyclic strength and pore pressure development. However, more research is needed to understand the dynamic response of compacted marginal soils in terms of cyclic resistance ratio (CRR) using field and lab data. Therefore, an attempt has been made in this study to evaluate the cyclic resistance of compacted marginal soil (clayey sand) by performing stress-controlled cyclic simple shear (CSS) tests in the laboratory and Standard Penetration Test (SPT) and Dynamic Cone Penetration Test (DCPT) in the field. The cyclic strength of marginal soil has been determined as Cyclic Resistance Ratio (CRR) by using laboratory (CSS) and field (SPT, DCPT) test data.

Keywords: cyclic stress ratio; cyclic resistance ratio; SPT; DCPT; cyclic simple shear

1. Introduction

In geotechnical infrastructure projects like highway embankments and retaining walls, clean, free-draining, non-plastic granular soils are preferred over fine-grained soils for their efficient performance (ASTM D3282-93 1993). The specific engineering properties that make coarse-grained soils suitable for these applications are good load-bearing capacity, high permeability, and better frictional resistance. The high permeability of such soil allows for efficient and quick drainage, preventing the buildup of excess pore water pressure, and, therefore, can be beneficial in applications where drainage and rapid dewatering are required. However, with time, a shortage of coarse-grained materials has occurred for various reasons, the most important of which are natural resource depletion, environmental concerns, and rising demand for construction and infrastructure development. This may result in the unavailability or scarcity of such desirable coarse-grained soils on or near the construction site. Considering the limited availability, high cost, and transportation issues associated with coarse-grained fill, the use of locally available marginal soils for various infrastructure projects is the need for today.

Marginal soils are lower quality, poorly draining soils with high fines content that can be cohesive or non-cohesive (Raja et al. 2019; Yang et al. 2016a; 2016b). The main concern regarding the use of marginal soils is the possibility of large evolution of positive pore water pressure, which may weaken the soil, resulting in a decrease in the shear strength (Yang et al. 2016a; 2016b). The marginal fills are often readily available and provide both economical and sustainable benefits; they are becoming a popular alternative to high-quality granular fill (Raja et al. 2019).

The increasing use of marginal soils in various major geotechnical infrastructure projects emphasizes the importance of studying their behaviour under different dynamic loading conditions to ensure the safety and stability of the structures built in or around such soil deposits. While loose saturated cohesionless soils such as clean sands and silty sands are the most prone to liquefaction, marginal soils containing fines are also known to lose strength and stiffness due to excess positive pore water pressure development during various types of dynamic or cyclic loading (Jayanandan and Viswanadham 2020; Hussain and Sachan 2019; 2020). The cyclic instability in clayey silt and clayey sand deposits during the Loma Prieta and Chi-Chi earthquakes, respectively, are pieces of evidence of the cyclic failure of fine-grained soils (Boulanger et al. 1997; Chu et al. 2004). Previous studies revealed cyclic strength reduction, pore pressure development, and stiffness degradation in soil deposits containing fines content under different dynamic loading conditions (Hussain and Sachan 2019; Okur and Ansal 2007). The effect of fines content, plasticity, and relative density on shear modulus and damping has also been studied by a few researchers (Shivaprakash and Dinesh 2017). However, the dynamic behaviour in terms of cyclic resistance ratio (CRR) using both field and laboratory data has not been studied for marginal soil deposits containing plastic fines. Exploring the dynamic response of such marginal soils with high water content, greater than the Optimum Moisture Content (OMC) of the soil, such as in the case of erratic rainfall, is also necessary for ensuring the efficient functionality and stability of structures built in or around such soil deposits.

In this study, CRR from field and lab data was determined and compared to study the dynamic behaviour of marginal soil of Palaj (Gandhinagar, India). Two types of field tests, Standard Penetration Test (SPT) and Dynamic Cone Penetration Test (DCPT) were conducted at 0.5 m depth at Palaj, Gandhinagar. The soil sample was collected from the same location and depth to conduct the cyclic simple shear (CSS) laboratory test. A series of stress-controlled Cyclic Simple Shear (CSS) tests was performed on compacted marginal soil specimens at different dynamic loading conditions. The cyclic resistance ratio (CRR) of marginal soil with plastic fines (Palaj soil) was calculated from all three tests: SPT, DCPT, and CSS to evaluate the dynamic response of marginal soil.

2. Material Properties

The soil sample was collected from Palaj, Gandhinagar (Gujarat, India) at a depth of 0.5 m from ground level. Grain size analysis revealed that the soil contained around 53% sand, 35% silt, and 12% clay. The soil had a specific gravity (G_s) of 2.67. The collected soil had a Liquid Limit (LL) of 26%, a Plastic Limit (PL) of 16%, and a Plasticity Index (PI) of 10%, according to the Atterberg limits assessment. The soil was classified as SC (Clayey Sand), as per the Indian Standard Classification System. Furthermore, the soil properties obtained from grain size analysis and Atterberg limits indicated that this soil could be termed as Marginal Soil. The detailed information regarding the geotechnical properties of Palaj soil is presented in Table 1.

Table 1 Geotechnical properties of Palaj soil

Properties	Values
Liquid Limit (LL)	26 %
Plastic Limit (PL)	16 %
Plasticity Index (PI)	10 %
Specific Gravity (G_s)	2.67
Sand	53 %
Silt (0.075 mm – 0.002 mm)	35 %
Clay (Finer than 0.002 mm)	12 %
Soil Classification	SC
Bulk Density (ρ)	1.88 g/cc
Maximum Dry Density (MDD)	1.92 g/cc
Optimum Moisture Content (OMC)	11%

3. Experimental Program and Specimen Preparation

SPT and DCPT field tests were conducted on marginal soil at 0.5 m depth in the Palaj soil site. The number of blows from SPT and DCPT were used to calculate the CRR values at 0.5 m depth of marginal soil strata in Palaj. The soil sample was collected from this location to conduct the cyclic simple shear (CSS) tests in the laboratory. A series of stress-controlled cyclic simple shear (CSS) tests were performed on compacted specimens of marginal soil under undrained conditions using the Norwegian Geotechnical Institute (NGI) type cyclic simple shear setup (ASTM D8296-19 2019). All the CSS tests were performed on cylindrical soil specimens of 70 mm diameter and 20 mm height at various Cyclic Stress Ratio (CSR) to evaluate the dynamic response of marginal soil (Palaj soil) under different dynamic loading conditions.

The CSS specimens were prepared in three equal layers using the moist tamping technique in a ring-type aluminium mould. The calculated amount of oven-dried soil was mixed with the required quantity of water to achieve a compacted soil specimen with a dry density of 1.79 g/cm^3 (93% MDD) and water content of 15% (3.8% greater than OMC). The unconfined compressive strength (q_u) of the specimens prepared at a moisture content higher than the OMC was determined to be 39 kPa, indicating its soft consistency. The prepared specimens were transferred to the pinned-type base pedestal assembly of Teflon-coated low-friction confining rings (ensuring a constant cross-sectional area) and a stretched latex membrane. The specimen, base pedestal assembly, and confining rings were mounted in an Electromechanical Dynamic Cyclic Simple Shear (EMDCSS) system. The CSS setup used in this study consisted of three (two shear and one axial) 5 kN load cells with a resolution of 0.1 N in horizontal and vertical directions, along with two axial and one horizontal LVDTs with a resolution of 0.1 m. After the assembly was set up, the specimen was docked and then subjected to saturation. The specimen was saturated by applying a seating pressure of 10 kPa and flushing out the de-aired water under a pressure of 1 m water head (Kantesaria and Sachan 2021). The volume of water flushed out was approximately 2-3 times that of the volume of the specimen. The saturated specimen was then consolidated under the K_o-condition at a vertical effective pressure (σ'_{vc}) of 100 kPa due to the rigid Teflon ring confinement around the specimen. The consolidation process took two to three hours. The specimen was then sheared under different dynamic loading conditions. The specimen volume was maintained constant during shearing to simulate the undrained boundary conditions during earthquake loading. The CSS tests were conducted at a cyclic loading frequency of 0.5 Hz and five different Cyclic Stress Ratios (CSRs) of 0.15, 0.162, 0.175, 0.2, and 0.25.

4. Results and Discussion

The current study is focused on the evaluation of the Cyclic Resistance Ratio (CRR) of marginal soil by conducting SPT, DCPT, and CSS tests. CRR was determined by conducting SPT and DCPT tests in the field and CSS tests in the laboratory. A series of CSS tests at different cyclic stress ratios (CSRs) was also conducted on compacted marginal soil specimens under different earthquake loading conditions by varying amplitude of stress-controlled, double-amplitude undrained cyclic loading during the shearing phase of the soil specimen.

4.1. CRR evaluation of marginal soil using SPT and DCPT field test data

The dynamic analysis of marginal soil was conducted using Standard Penetration Test (SPT) and Dynamic Cone Penetration Test (DCPT) field data. Subsequently, the in-situ test parameters (number of blows from SPT and DCPT) were obtained to calculate the cyclic resistance ratio (CRR). The dynamic cone resistance (N_{cd}) was first converted into SPT N value and then analyzed for cyclic instability resistance following the same procedure as the Standard Penetration Test. For a depth of 0.5 m (< 3 m) and a cone diameter of 50 mm, the correlation between N_{cd} and N used in this study was $N_{cd} = 1.5N$ (Ranjan and Rao 2011). The recorded standard penetration resistance from field tests being influenced by the overburden pressure, a correction factor C_N was used to normalize the SPT N value to a common reference effective overburden stress. This factor was chosen based on the overburden stress present during testing following IS 2131:1981 2016. The factor of safety (FS) against cyclic instability was determined and listed in Table 2. The peak ground acceleration (a_{max}) was set at 0.16 times the acceleration due to gravity (g), taking into account the location in Seismic Zone III as per the Indian seismic code IS 1893: 2016 (2016). A design earthquake magnitude (M_w) of 7.5 was adopted. In this field data analysis, the seismic demand was represented as cyclic stress ratio (CSR), and the soil's ability to resist the applied seismic stress was expressed as cyclic resistance ratio (CRR). FS is the ratio of CRR and CSR. All the critical variables of this in-situ data analysis were calculated using the methodology outlined in Youd et al. 2001. All the analysis and related parameters are listed in Table 2. The factor of safety (FS) was determined to be greater than 1 for both SPT (FS = 2.6) and DCPT (FS = 3.1), which exhibited the absence of liquefaction in Palaj soil. This could be attributed to the substantial presence of plastic and non-plastic fines content in the Palaj soil deposits. The CRR value was obtained to be more for DCPT than SPT, exhibiting larger cyclic resistance of Palaj soil at 0.5 m depth for DCPT than SPT.

Table 2 Factor of safety against liquefaction obtained based on SPT and DCPT tests

Parameters	In-situ Tests Performed	
	SPT	DCPT
Number of Blows	N value = 8	N_{CD} value = 14
CRR	0.265	0.325
CSR	0.104	0.104
FS	**2.6**	**3.1**

4.2. CRR evaluation of marginal soil using CSS lab test data

A series of CSS tests were performed on compacted marginal soil specimens at different CSR values to evaluate the cyclic resistance ratio (CRR) of marginal soil. Hysteresis loops of marginal soil were obtained at different CSR values, indicating different earthquake loading conditions. The cyclic strength characteristics of soil were determined through these hysteresis loops. The cyclic stress-strain behaviour during two-way stress-controlled undrained cyclic loading is illustrated in Fig. 1. A decrease in the number of cyclic loops was observed as the cyclic stress ratio (CSR) increased from 0.15 to 0.25. The results exhibited that an increase in CSR resulted in a sharp rise in shear strain within a limited number of loading cycles (Fig. 2). This caused a significant reduction in the cyclic resistance and load-carrying capacity of the marginal soil.

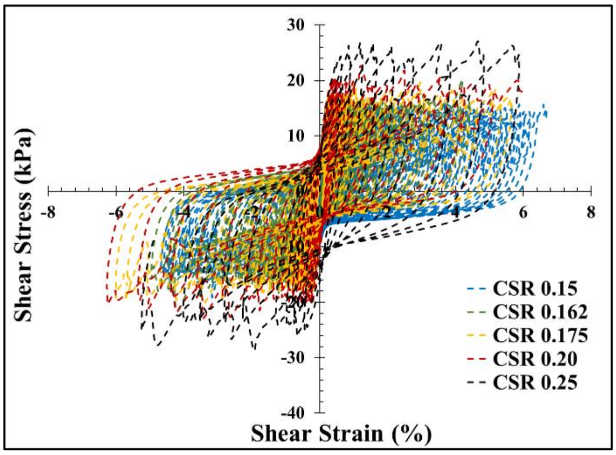

Fig. 1 Hysteresis loops corresponding to different CSRs

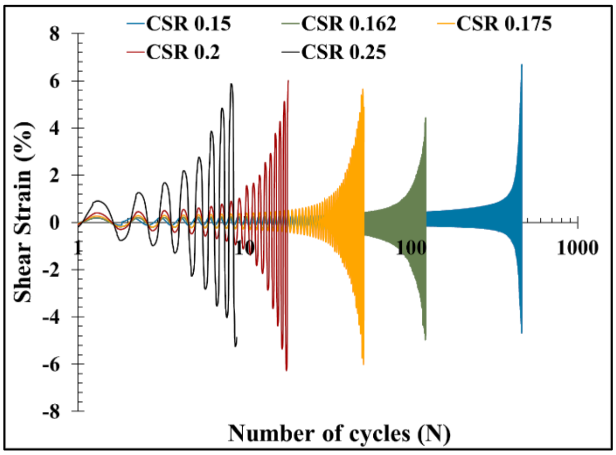

Fig. 2 Shear strain development with the number of cycles corresponding to different CSRs

During undrained cyclic loading conditions, an increase in the pore water pressure was observed due to an increase in the amplitude of cyclic loading. The pore water pressure at any given time comprises two components: a residual component and a cyclic component. Residual pore water pressure is the portion of the excess pore water pressure that remains within the soil structure after cyclic loading has stopped. This is attributed to plastic deformation induced by the cyclic stress-strain history. On the other hand, the cyclic component represents the instantaneous increment caused by alterations in either the mean normal stress or the shear stresses (Siddharthan and Norris 1990). An understanding of how these pore water pressures develop and dissipate is crucial for assessing the potential for post-earthquake settlement, stability concerns, and other geotechnical considerations. Fig. 3 exhibits the development of excess positive pore water pressure in the soil specimens with increasing loading cycles (N) under different dynamic loading scenarios. With the application of increasing CSR values under the same effective confining pressure and the same loading frequency, the rate of generation of excess pore water pressure in the soil specimen increased.

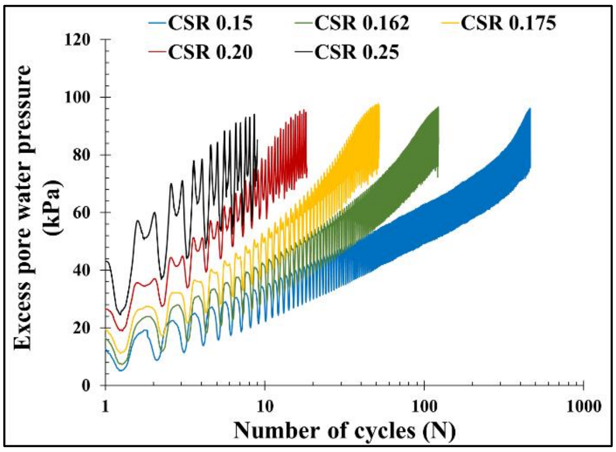

Fig. 3 Excess pore water pressure developed with the number of cycles corresponding to different CSRs

The excess pore water developed within the soil mass can be expressed in terms of the pore pressure ratio (r_u), defined as the ratio of the generated excess pore water pressure to the initial vertical effective stress applied to the soil. For a better illustration, the evolution of excess pore water pressure during cyclic loading is presented in terms of maximum pore pressure ratio ($r_{u,\ max}$) and residual pore pressure ratio ($r_{u,\ res}$) over an increasing number of loading cycles, as depicted in Figs. 4(a) and 4(b) respectively. When the cyclic stress ratio (CSR) was low, a gradual increase in both $r_{u,\ max}$, and $r_{u,\ res}$ was observed with increasing loading cycles, culminating in failure eventually after a large number of loading cycles. In contrast, higher amplitudes of cyclic stresses (CSR = 0.175, 0.2, 0.25) were found to lead to rapid and significant amplitude of pore pressure accumulation within a limited number of initial loading cycles.

The change in pore pressure ratio (r_u) in compacted marginal soil under stress-controlled conditions was obtained with respect to both shear strain and number of loading cycles (Fig. 5). It can be observed that while maintaining a constant amplitude of deviatoric stress, there was a continuous evolution in the pore pressure ratio (r_u). This ongoing pore pressure evolution subsequently gave rise to a progressive increase in shear strains, which ultimately caused instability and cyclic failure within the soil mass.

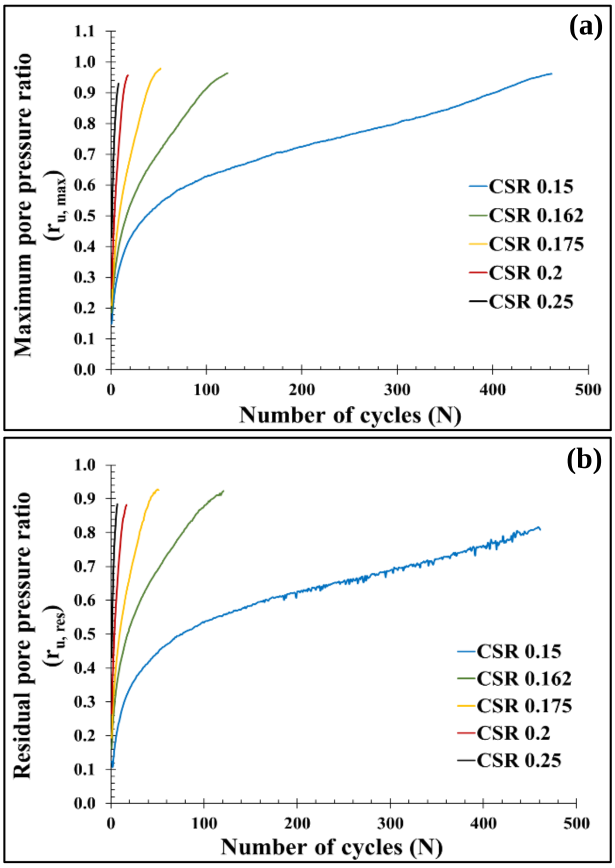

Fig. 4 (a) Maximum pore pressure ratio (b) Residual pore pressure ratio variation with the number of cycles corresponding to different CSRs

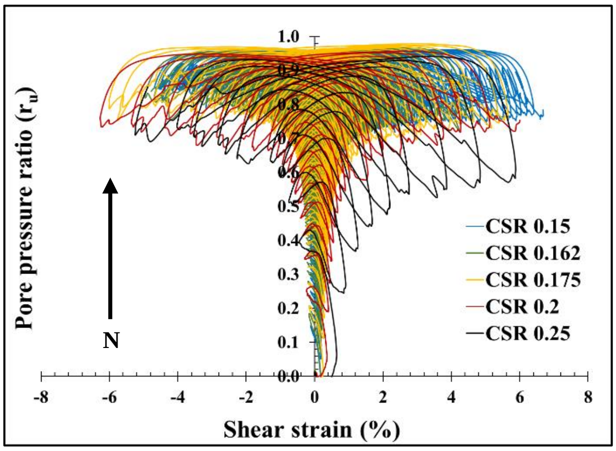

Fig. 5 Pore pressure ratio variation with shear strain and number of loading cycles corresponding to different CSRs

Shear modulus (G) and damping ratio (D) were calculated for each loading cycle of all the CSS tests corresponding to the CSR values ranging from 0.15 to 0.25. The variation in shear modulus with increasing loading cycles and cyclic stress amplitudes was presented using the concept of cyclic degradation index (δ). The cyclic degradation index is defined as the ratio of the shear modulus at the N^{th} cycle (G_N) to the shear modulus at the 1^{st} cycle (G_0) ($\delta = \frac{G_N}{G_0}$). The change in cyclic degradation index (δ) with the number of cycles (N) for different cyclic stress ratios (CSRs) was also evaluated (Fig. 6). The soil stiffness was found to diminish as the number of loading cycles (N) increased. The acceleration in the rate of stiffness degradation was also observed with the increase of cyclic loading stress amplitudes. The highest stiffness degradation was observed in the specimen subjected to the highest CSR. The lower values of the cyclic degradation index exhibited a larger magnitude of stiffness degradation. The variation in the damping ratio with the number of loading cycles (N) for different cyclic stress ratio (CSR) values is shown in Fig. 7. Initially, a minor change in the damping ratio was observed with the increase in the number of loading cycles (N). This could be attributed to the initiation of fatigue at higher loading cycles, wherein the specimen underwent an excessive rise in pore water pressure. This led to a large decrease in effective stress and corresponding cyclic failure. A loss of bonding and frictional resistance among the soil particles at higher loading cycles resulted in a more pronounced energy dissipation and subsequent increase in the damping ratio. However, a clear pattern of this behaviour was not distinctly observed for the CSR value of 0.25. This could be due to the rapid development of excess pore water pressure and energy loss in the soil specimen within a limited number of initial loading cycles.

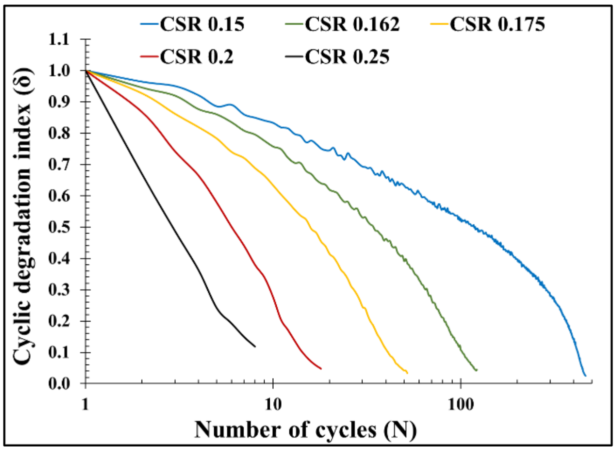

Fig. 6 Cyclic degradation index with the number of cycles corresponding to different CSRs

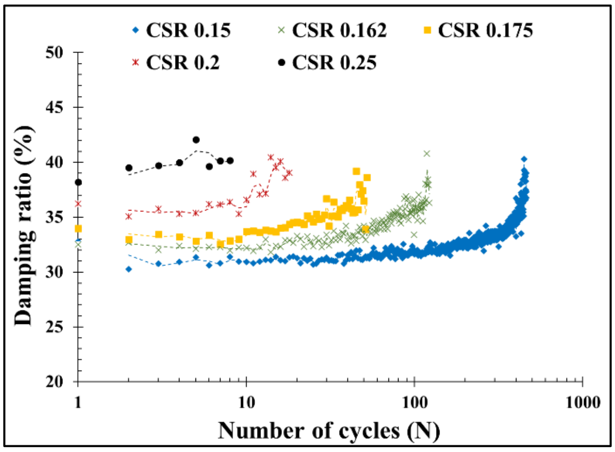

Fig. 7 Damping ratio variation with the number of cycles corresponding to different CSRs

The double amplitude shear strain was evaluated for each loading cycle corresponding to CSR values ranging from 0.15 to 0.25. It is the strain obtained by dividing the peak-to-peak horizontal displacement by the specimen height. The variation of the double amplitude shear strain with the number of loading cycles corresponding to different CSR values is presented in Fig. 8. The double amplitude shear strain was observed to gradually increase with an increasing number of loading cycles. An abrupt rise in the double amplitude strain was further noted after a certain number of loading cycles corresponding to every CSR value of 0.15 to 0.25. This resulted in a significant loss of cyclic resistance within the soil mass. A greater double amplitude shear strain was observed to develop in the soil specimen within a relatively smaller number of loading cycles as the cyclic stress loading amplitude increased.

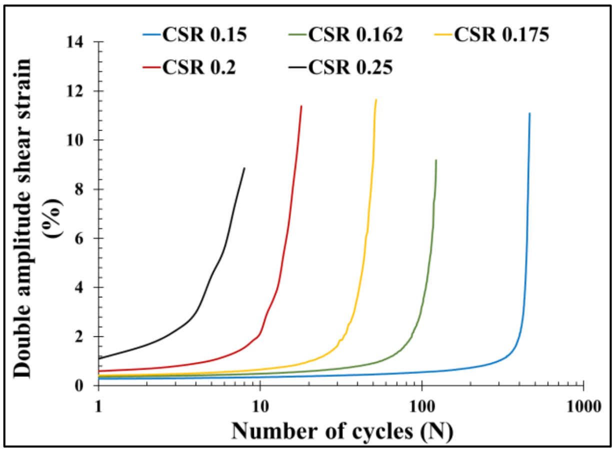

Fig. 8 Double amplitude shear strain variation with the number of cycles corresponding to different CSRs

In this study, the cyclic failure of soil was defined using the concepts of both double amplitude shear strain and maximum pore pressure ratio ($r_{u,\ max}$). The loss of cyclic resistance in the soil was considered to occur either when the double amplitude shear strain of 7.5% was exceeded (Pillai and Stewart 1994) or when the maximum pore pressure ratio of 0.85 was exceeded (Beaty and Byrne 2011). The number of loading cycles required to initiate cyclic failure (N_L) corresponding to $r_{u,\ max}$ of 0.85, and double amplitude shear strain of 7.5% are listed in Table 3. The Cyclic Resistance Ratio (CRR) is equivalent to the Cyclic Stress Ratio (CSR) at 15 number of loading cycles (Seed et al. 1975). The CRR was determined using the best-fit line of the cyclic resistance curves (Fig. 9). The CRR values corresponding to $r_{u,\ max}$ of 0.85, and a double amplitude strain of 7.5% were found to be 0.209 and 0.214, respectively. The minimum of the CRR values was then used to define the cyclic resistance of the soil.

Thus, in summary, the CSS testing of the soil compacted with a moisture content exceeding the Optimum Moisture Content (OMC) resulted in a Cyclic Resistance Ratio (CRR) of 0.209. However, field tests such as SPT and DCPT indicated higher CRR values of 0.265 and 0.325, respectively, under in-situ conditions. The discrepancy in CRR values between CSS and field tests was likely due to changes in the soil's microstructure during wet compaction in the laboratory compared to its natural state at the Palaj site. Moreover, the higher moisture content in the compacted soil specimens led to decreased resistance to cyclic instability.

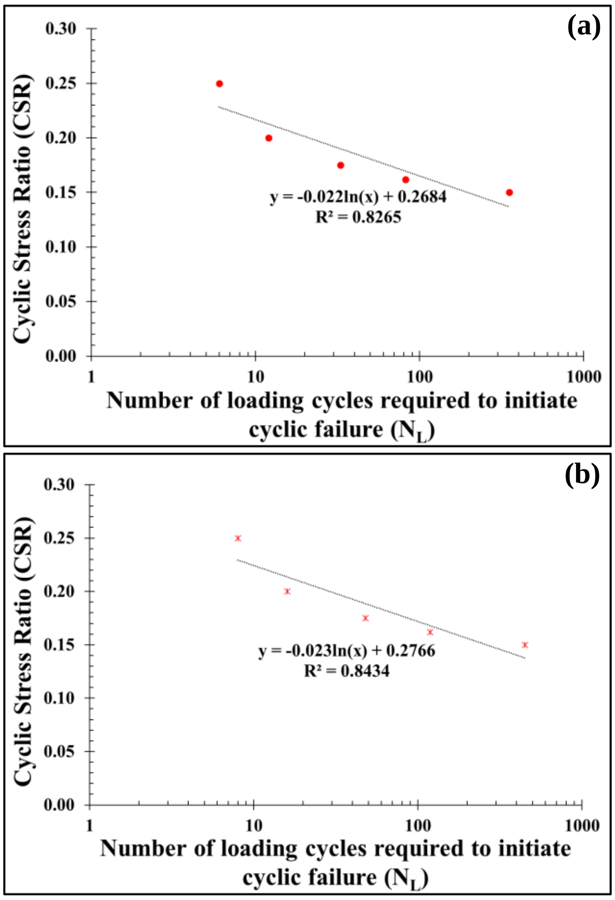

Fig. 9 Cyclic resistance curves corresponding to (a) Maximum pore pressure ratio of 0.85 (b) Double amplitude shear strain of 7.5%

Table 3 N_L corresponding to $r_{u,\ max}$ of 0.85, and double amplitude shear strain of 7.5%

CSR	N_L corresponding to maximum r_u of 0.85	N_L corresponding to Double Amplitude Shear Strain of 7.5%
0.150	352	450
0.162	82	119
0.175	33	48
0.200	12	16
0.250	6	8

5. Conclusions

The current study was focused on the evaluation of the dynamic behaviour of marginal soil in terms of cyclic resistance ratio (CRR) using both field and laboratory test data. The cyclic resistance ratio (CRR) of marginal soil was calculated at its in-situ conditions using SPT and DCPT field test data and at compacted state using CSS lab data. The following major conclusions can be drawn from the current study –

1. The shear strain was found to accumulate at a lesser number of loading cycles as the CSR increased. This indicated that the cyclic resistance of the soil decreased as the cyclic loading amplitude increased.

2. The amplitude of excess pore water pressure was observed to progressively increase with the number of loading cycles at lower CSR values, eventually causing failure or instability. In contrast, a faster and larger accumulation of pore water pressure was found to occur within a few cycles at the beginning of the test when the CSR was high.

3. A significant degradation of shear modulus with the number of loading cycles was observed corresponding to each CSR from 0.15 to 0.25. This indicated a significant reduction in soil strength and stiffness with increasing CSR values. The rate of stiffness degradation was also found to increase with an increase in the loading amplitude.

4. In the first ten loading cycles, the damping ratio was observed to increase with the increase in CSR values.

5. Cyclic failure or cyclic instability of compacted marginal soil under various dynamic loading scenarios with undrained boundary conditions was indicated by (a) a double amplitude shear strain of 7.5% (even if $r_{u,\ max} < 0.85$) or (b) shear strain at which $r_{u,\ max} = 0.85$, whichever is lower. In this study, the CRR corresponding to $r_{u,\ max}$ was identified as the minimum and was subsequently used to define the cyclic resistance of the soil subjected to dynamic loading.

6. CRR of marginal soil deposit at in-situ conditions was obtained to be 0.265 and 0.325 using SPT and DCPT data, respectively. However, the CRR of compacted marginal soil in the laboratory was determined to be 0.209, which was much smaller than the field results.

Acknowledgements

The author expresses heartfelt gratitude to the esteemed Indian Institute of Technology Gandhinagar, Gandhinagar, for their generous financial support, which played a pivotal role in the realization of this work. Additionally, the author extends sincere appreciation for the invaluable technical support extended by the institute. It is important to note that any perspectives, discoveries, and conclusions articulated in this manuscript are solely the reflections of the authors and do not necessarily mirror the perspectives of IIT Gandhinagar.

References

ASTM D8296-19. 2019. "Standard Test Method for Consolidated Undrained Cyclic Direct Simple Shear Test under Constant Volume with Load Control or Displacement Control." *ASTM International*, no. November.

ASTM D3282-93. 1993. "Standard Practice for Classification of Soils and Soil-Aggregate Mixtures for Highway Construction Purposes." ASTM International.

Beaty, M. H., and P. M. Byrne. 2011. "UBCSAND Constitutive Model, Version 904aR." Itasca UDM Web Site.

Boulanger, R. W., L. H. Mejia, and I. M. Idriss. 1997. "Liquefaction at Moss Landing during Loma Prieta Earthquake." Journal of Geotechnical and Geoenvironmental Engineering 123 (5). https://doi.org/10.1061/(asce)1090-0241(1997)123:5(453).

Chu, D. B., J. P. Stewart, S. Lee, J. S. Tsai, P. S. Lin, B. L. Chu, R. B. Seed, S. C. Hsu, M. S. Yu, and M. C. H. Wang. 2004. "Documentation of Soil Conditions at Liquefaction and Non-Liquefaction Sites from 1999 Chi-Chi (Taiwan) Earthquake." Soil Dynamics and Earthquake Engineering 24 (9–10). https://doi.org/10.1016/j.soildyn.2004.06.005.

Hussain, M., and A. Sachan. 2019. "Dynamic Characteristics of Natural Kutch Sandy Soils." Soil Dynamics and Earthquake Engineering 125. https://doi.org/10.1016/j.soildyn.2019.105717.

Hussain, M., and A. Sachan. 2020. "Dynamic Behaviour of Kutch Soils under Cyclic Triaxial and Cyclic Simple Shear Testing Conditions." International Journal of Geotechnical Engineering 14 (8). https://doi.org/10.1080/19386362.2019.1608715.

IS 1893 : 2016. 2016. "Criteria for Earthquake Resistant Design of Structures, Part 1:General Provisions and Buildings." Bureau of Indian Standards, New Delhi 1893.

IS 2131:1981. 2016. “Method for Standard Penetration Test for Soils.” Bureau of Indian Standards.

Jayanandan, M., and B. V. S. Viswanadham. 2020. "Geogrid Reinforced Soil Walls with Marginal Backfills Subjected to Rainfall: Numerical Study." Indian Geotechnical Journal 50 (2). https://doi.org/10.1007/s40098-019-00396-0.

Kantesaria, N., and A. Sachan. 2021. "Cyclic Degradation and Pore-Water Pressure Response of High-Plasticity Compacted Clay." Journal of Geotechnical and Geoenvironmental Engineering 147 (11). https://doi.org/10.1061/(asce)gt.1943-5606.0002630.

Okur, D. V., and A. Ansal. 2007. "Stiffness Degradation of Natural Fine Grained Soils during Cyclic Loading." Soil Dynamics and Earthquake Engineering 27 (9). https://doi.org/10.1016/j.soildyn.2007.01.005.

Pillai, V. S., and R. A. Stewart. 1994. "Evaluation of Liquefaction Potential of Foundation Soils at Duncan Dam." Canadian Geotechnical Journal 31 (6). https://doi.org/10.1139/t94-110.

Raja, J., N. Dixon, M. Frost, and I. Fraser. 2019. "Designing with Marginal Fills : Understanding and Practice." International Geosynthetics Society(IGS) 5.

Ranjan, G., and Rao, A. S. R. (2011). Basic and applied soil mechanics. New Age International.

Seed, H. B., I. M. Idriss, F. Makdisi, and N. Banerjee. 1975. "Representation of Irregular Stress Time Histories by Equivalent Uniform Stress Series in Liquefaction Analyses." Earthquake Engineering Research Center.

Shivaprakash, B. G., and S. V. Dinesh. 2017. "Dynamic Properties of Sand–Fines Mixtures." Geotechnical and Geological Engineering 35 (5). https://doi.org/10.1007/s10706-017-0247-3.

Siddharthan, R., and G. M. Norris. 1990. "Residual Porewater Pressure and Structural Response." Soil Dynamics and Earthquake Engineering 9 (5). https://doi.org/10.1016/S0267-7261(05)80005-3.

Yang, K. H., M. D. Nguyen, W. M. Yalew, C. N. Liu, and R. Gupta. 2016a. "Behavior of Geotextile-Reinforced Clay in Consolidated-Undrained Tests: Reinterpretation of Porewater Pressure Parameters." Journal of GeoEngineering 11 (2). https://doi.org/10.6310/jog.2016.11(2).1.

Yang, K.-H., W. M. Yalew, and M. D. Nguyen. 2016b. "Behavior of Geotextile-Reinforced Clay with a Coarse Material Sandwich Technique under Unconsolidated-Undrained Triaxial Compression." International Journal of Geomechanics 16 (3). https://doi.org/10.1061/(asce)gm.1943-5622.0000611.

Youd, T. L., I. M. Idriss, R. D. Andrus, I. Arango, G. Castro, J. T. Christian, R. Dobry, et al. 2001. "Liquefaction Resistance of Soils: Summary Report from the 1996 NCEER and 1998 NCEER/NSF Workshops on Evaluation of Liquefaction Resistance of Soils." Journal of Geotechnical and Geoenvironmental Engineering 127 (10). https://doi.org/10.1061/(asce)1090-0241(2001)127:10(817).